Optik - International Journal for Light and Electron Optics 287 (2023) 171059

Contents lists available at ScienceDirect

Optik

journal homepage: www.elsevier.com/locate/ijleo

Original research article

SIPAM-4 scheme improves bit error rate performance in MISO X-ray communication system

Feixu Xiong [a], Yunpeng Liu [a,b,*], Junqiu Yin [a], Junxu Mu [a], Xiaobin Tang [a,b,*]

[a] Department of Nuclear Science and Technology, Nanjing University of Aeronautics and Astronautics, Nanjing 210016, China
[b] Key Laboratory of Nuclear Technology Application and Radiation Protection in Astronautics, Ministry of Industry and Information Technology, Nanjing 210016, China

ARTICLE INFO

Keywords:
X-ray communication
Superimposed intensity
Pulse amplitude modulation
MISO
Grid-modulated X-ray tube

ABSTRACT

X-ray communication (XCOM) technology, which uses X-ray as the carrier wave, is expected to solve the problem of reentry blackout region communication with its good penetration characteristics. In order to mitigate the effects of non-linear distortion of the gated X-ray tube (GMXT), the multiple-input single-output (MISO) technique has been introduced in XCOM systems. A pulse amplitude modulation scheme based on superimposed intensity (SIPAM) was proposed and achieved by configuring GMXTs with on/off keying modulation in MISO XCOM system. The feasibility of the proposed SIPAM scheme in XCOM was numerically investigated through Monte Carlo simulations. As the divergence angle of the GMXT increases, the optical power distribution tends to be more uniform in the receiving plane. It can greatly relax the requirements for link alignment. After that, we conduct a proof-of-concept experiment for the SIPAM with four levels (SIPAM-4) scheme by employing two GMXTs and an LYSO-SiPM-based X-ray detector. The experimental results show that when the bit error rate is within the forward error correction limit of 3.8×10^{-3}, the SIPAM-4 scheme can reach a maximum communication rate of 1.20 Mbps, which is 20% higher than the conventional PAM-4 scheme. It can be included that the proposed MISO based the SIPAM-4 modulation scheme could improve the performance of the X-ray communication system.

1. Introduction

X-ray communication (XCOM) is a wireless optical communication technology that uses X-ray as a data transmission carrier. The photons of X-ray have the characteristics of short wavelength and strong penetrating power, and are highly resistant to electromagnetic fields and high-energy particles. X-ray beams with energy higher than 10 keV ($\lambda < 0.1$ nm) can be transmitted almost without attenuation in environments with atmospheric pressure below 10^{-1} Pa [1], which means that XCOM is able to transmit data over long distances in deep space environments. In addition, it was demonstrated that X-ray are transmitted almost without attenuation in a plasma environment with electron density of 10^{9}-10^{14}/cm^{3} [2,3], which indicates that XCOM is expected to solve the communication problem in the reentry blackout region. Compared with the conventional communication technology, the XCOM scheme using X-ray as the carrier wave is more feasible in special environments such as deep space and the reentry blackout region.

* Corresponding authors at: Department of Nuclear Science and Technology, Nanjing University of Aeronautics and Astronautics, Nanjing 210016, China
E-mail addresses: liuyp@nuaa.edu.cn (Y. Liu), tangxiaobin@nuaa.edu.cn (X. Tang).

https://doi.org/10.1016/j.ijleo.2023.171059
Received 19 November 2022; Received in revised form 22 May 2023; Accepted 6 June 2023
Available online 8 June 2023

A typical X-ray communication system is composed of a transmitter/receiver of X-ray signals, a modulation and demodulation module, and a collimated focusing module, as shown in Fig. 1. The existing XCOM system is a single-input single-output (SISO) system [4,5]. The main modulated X-ray sources used at the transmitter side are the grid-modulated X-ray tube (GMXT), photocathode X-ray sources, and the field emission X-ray sources. Among them, the GMXT is commonly used as a transmitter in XCOM due to its mature technology. The data to be transmitted is loaded onto the gate of the GMXT by a modulator that controls the on/off flow of electrons to produce modulated X-rays. The modulated X-rays is then collimated and transmitted in the channel environment. X-rays are detected by the detector module after focusing and finally reduced by the demodulator module.

In XCOM, the X-ray generated by electron targeting is poor in its monochromaticity. Therefore, the data transmission of current XCOM systems is realized by the intensity modulation/direct detection (IM/DD) technique, which uses X-ray intensity to transmit information. The general candidates for data modulation in existing XCOM studies are single-carrier pulse modulation schemes such as on/off keying (OOK) modulation and pulse position modulation (PPM). Although these conventional modulation techniques are simple and easy to implement, their spectrum utilization and communication rate are low. Zhou et al. [6] proposed a transmission link model for XCOM systems and investigated the relationship between the signal-to-noise ratio and bit error rate (BER) of XCOM links under different modulation methods, including OOK and PPM. Wang et al. [7] showed that at a 25 kbps data rate, the BER of OOK and PPM is about 10^{-4}. Orthogonal frequency division multiplexing (OFDM) has been investigated in XCOM, and Chen et al. [8] experimentally demonstrated a modified OFDM-to-PWM scheme for XCOM to reach 360 kbps at a forward error correction (FEC) threshold of 3.8×10^{-3} for a BER kbps data rate, although increasing the system complexity to some extent [9–11]. Pulse amplitude modulation (PAM) has attracted much attention due to its high spectral efficiency, low computational complexity, and ease of implementation [12,13]. However, studies [14] have shown that generating a conventional PAM signal requires a signal source with good linearity. For XCOM, the relationship between the gate voltage of the transmitter GMXT and the intensity of the emitted X-ray is nonlinear [8,15], which will severely limit the data rate. To obtain better communication performance, the modulation amplitude of the PAM signal should be within the linear range of the GMXT.

In order to mitigate the effects of nonlinearity at the transmitter side and improve the communication rate, it is necessary to go for a new and efficient modulation technique. The rest of the paper is organized as follows: In Section 2, the XCOM system, GMXT characteristics, detector, and modulation principles are introduced. In Section 3, the feasibility of the modulation scheme and the effect of the divergence angle on the power distribution were simulated. In Section 4, the effects of operating parameters such as data transmission rate, anode voltage, and distance on the BER of the system were experimentally investigated. Finally, conclusions are given in Section 5.

2. XCOM and modulation principles

2.1. MISO XCOM system

How to solve the nonlinear distortion to enhance the communication rate and reduce system complexity has become the main problem of X-ray tube modulation technology. In the field of visible light communication, a spatial modulation (SM) technique has been proposed for similar problems, using multiple-input single-output (MISO) systems instead of SISO systems [16–18]. In order to address the effects of nonlinearity at the transmitter side of the XCOM system, we started an in-depth study of the spatial characteristics of the array X-ray source and introduced MISO's XCOM system. Multiple GMXTs are arranged at the transmitter side to achieve multi-stage modulation by optical superposition in order to improve the spectral efficiency while resisting the modulation nonlinearity of GMXT. Taking the XCOM system of 2×1 MISO as an example, it mainly consists of a upper/lower computer, FPGA, power amplifier, two GMXTs, and a detector, and the system schematic is shown in Fig. 2.

2.2. GMXT characteristics

The GMXT is mainly composed of a hot cathode, a gate, an anode target, and a tube shell, and its structure is schematically shown in Fig. 3(a). In XCOM, the GMXT changes the spatial electric field distribution by adding a negative polarity voltage signal to the gate and controls the number of electrons bombarding the anode target by the electric field, thus changing the intensity of the emitted X-ray and realizing the signal loading of X-ray (Fig. 3(b)).

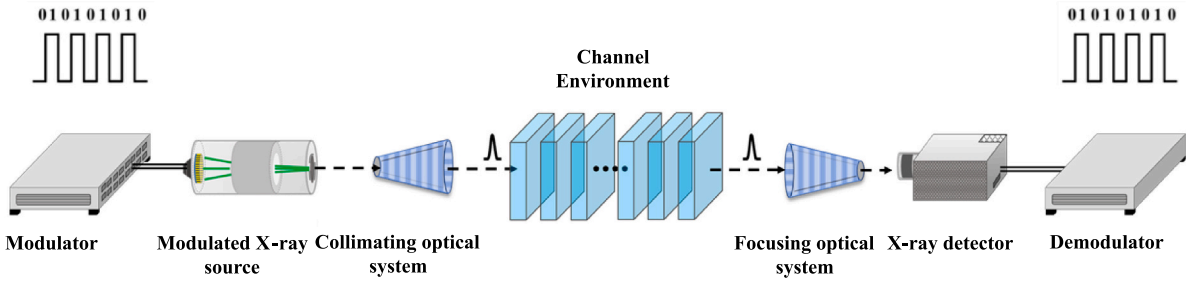

Fig. 1. Schematic diagram of X-ray communication system.

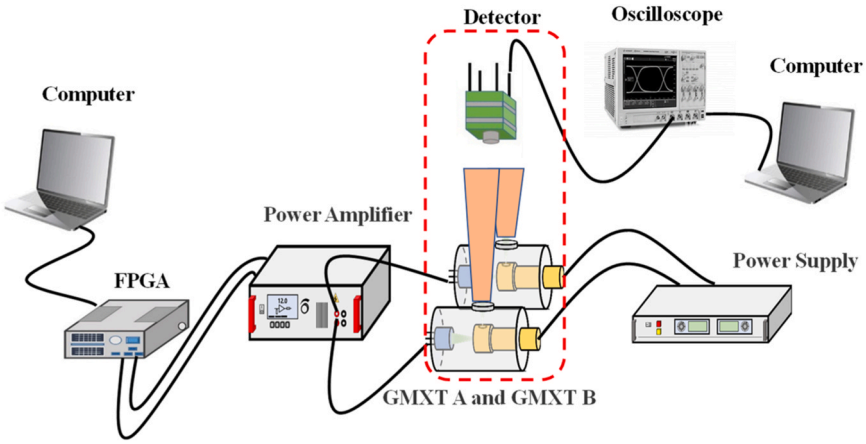

Fig. 2. Schematic diagram of MISO X-ray communication system.

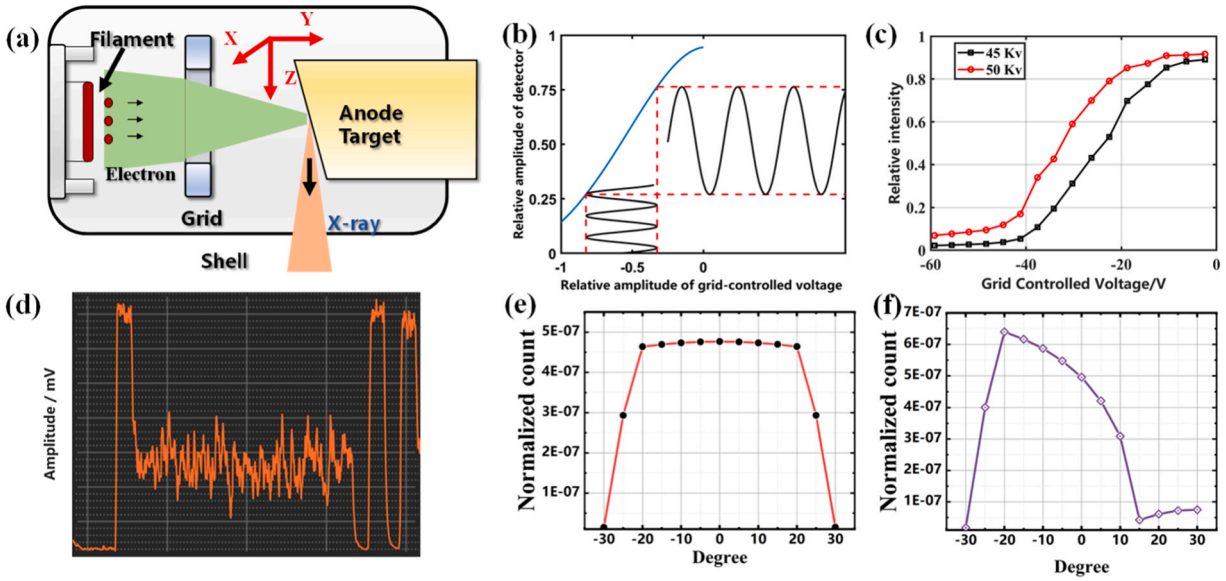

Fig. 3. (a) Schematic diagram of GMXT. (b) Principle of signal loading in XCOM. (c) Relationship between gate voltage and output X-ray intensity at different anode voltages (experimental measurements). (d) Amplitude dithering of the waveform. spatial distribution of X-ray on (e) X-axis and (f) Y-axis.

The curve of gate voltage versus intensity of the emitted X-ray for the GMXT is shown in Fig. 3(c). For higher-order PAM schemes, when the amplitude of the gate control voltage is too large or too small, the signal enters the nonlinear region, and distortion and BER will occur. Moreover, the intensity of the emitted X-ray will fluctuate even in the relatively linear operating range (Fig. 3(d)), which will reduce the signal-to-noise ratio of the signal. In addition, the X-ray produced by the reflective X-ray tube have an asymmetric spatial distribution (Fig. 3(e) and (f)). Here, the normalized photon count represents the average of the X-ray counts produced by accelerated electrons, and its value characterizes the number of emitted X-ray photons.

2.3. X-ray detector

The X-ray detector consists of a lutetium yttrium silicate scintillator (LYSO) scintillator and a silicon photomultiplier (SiPM). The LYSO scintillator converts the received X-ray into visible light with a central wavelength of about 420 nm, which is coupled to the SiPM module at the fluorescent photon-emitting side of the LYSO to convert the visible light signal into an electrical signal.

2.4. Modulation principles

In this study, we proposed a scheme to achieve higher-order pulse amplitude modulation using intensity superposition (SIPAM). It

was assumed that there are N GMXTs at the transmitter side, all modulated by OOK, and their outgoing X-ray intensities are A, A/2,., A/2 $^{N-1}$. When the N GMXTs operate synchronously and emit X-ray, the emitted X-ray will be superimposed in free space. Then a SIPAM-2 N modulated signal is generated, which has an N-times higher transmission rate than OOK and is resistant to nonlinear distortion. The SIPAM signal y can be expressed by the following equation:

$$y = \sum_{k=1}^{N} \frac{A * \delta(k)}{2^{k-1}}$$

where A is the maximum intensity of the GMXT and $\delta(k)$ indicates whether the kth GMXT emits X-ray or not, "1" means it emits X-ray, and "0" means it does not emit X-ray.

The two GMXTs emit X-ray OOK signals with an intensity ratio of 2:1, and when the two OOK signals are emitted simultaneously, they are superimposed in the intensity domain during transmission to generate SIPAM-4 signals (Fig. 4).

2.5. Design on research scheme

In order to verify the performance of the SIPAM scheme, two parts, simulation and experiment, were designed. In the simulation part, the feasibility of the SIPAM scheme was investigated by using the Monte Carlo software Geant4 to investigate the effect of the divergence angle of the GMXT on the X-ray power distribution and power ratio at the receiving end. In the experimental part, a dual-transmitter single-receiver XCOM system was built in the laboratory, and finally the SIPAM-4 scheme was tested on the built platform. By comparing the BER of SIPAM-4 and PAM-4 under different operating conditions, the improvement effect of SIPAM on the communication performance of XCOM system was evaluated.

3. Simulation and results

3.1. Simulation model and parameter configuration

The transport process of X-ray was simulated using the Monte Carlo software Geant4, and the numerical simulations investigated the feasibility of MISO-XCOM and the effect of the divergence angle on the optical power distribution at the receiving surface. The configuration of the array is flexible, so we chose the most common fixed pitch interleaved array. In the simulations, an array with 4 × 4 GMXTs, which was divided into two uniformly interwoven groups A and B, was used (Fig. 5(a)). The spacing of each of the two adjacent GMXTs in the array was assumed to be 4 cm. The diameter of the emitting surface of the X-ray source was assumed to be 1.5 cm. The dispersion angle and energy of the GMXTs are 90° and 30 keV, respectively. The spatial distribution of the emitted X-ray is shown in Fig. 3(e) and (f). The transmission model of the array XCOM system is shown in Fig. 5(b). An X-ray detector was placed 100 cm away from the GMXT array with a field of view of 180° ($\psi = 90°$) to record the position and energy of the arriving X-ray. The intensity ratio (i.e., power ratio) P_A: P_B of light sources A and B was assumed to be 1:3.

3.2. Simulation results and discussion

Fig. 6(a) shows the superimposed X-ray power distribution at the receiver after 100 cm of free air. Fig. 6(b) represents the X-ray power ratio P_A:$P_B \approx$ 1:3 in the overlapped region, which is closed to the configured intensity ratio of the source. The uniform power ratio verifies the feasibility of the proposed intensity superposition scheme and ensures that the PAM signal can be generated at the receiving end. Meanwhile, since the conventional SISO XCOM system requires point-to-point alignment to achieve good performance in the communication process, the uniform power ratio distribution at the receiver end for the array transmitter system means that the detector alignment requirement can be relaxed in the actual communication process, which improves the reliability of XCOM.

In addition, the effect of GMXTs with different divergence angles on the optical power distribution was investigated. The simulation results are shown in Fig. 7. When the divergence angle of GMXT increases from 25° to 60°, the power distribution in the detection plane

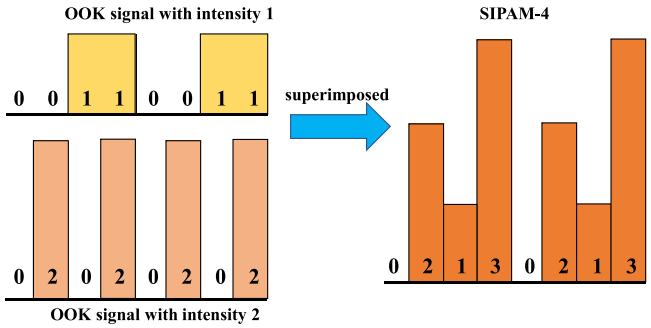

Fig. 4. Schematic diagram of SIPAM-4.

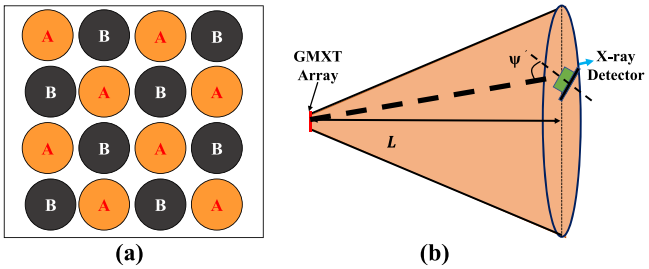

Fig. 5. (a) An GMXT array and (b) XCOM system model.

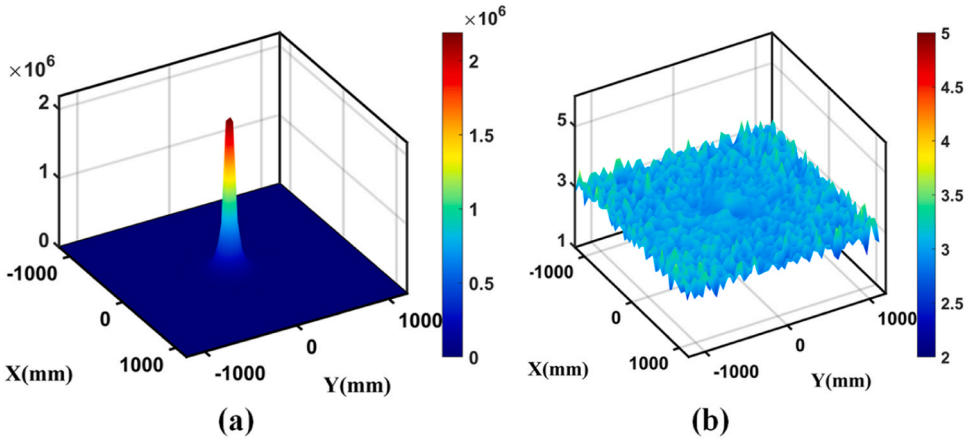

Fig. 6. (a) Power distribution of receiving plane. (b) The power ratio of X-ray sources in groups A and B.

at the receiver side gradually tends to be uniformly distributed, which relaxes the requirement for link alignment in practical applications.

Although the X-ray distribution emitted by GMXT was asymmetric, the distribution of X-ray at the receiving end was approximately uniform due to the evenly staggered multiple GMXTs. This arrangement increases the robustness of the system. The more the number of X-ray tubes, the more the system's robustness.

4. Experiment and results

4.1. Experimental setup

Fig. 8 shows the structure of the 2 × 1 MISO XCOM system, which was utilized in the experiments to validate the SIPAM-4 scheme.

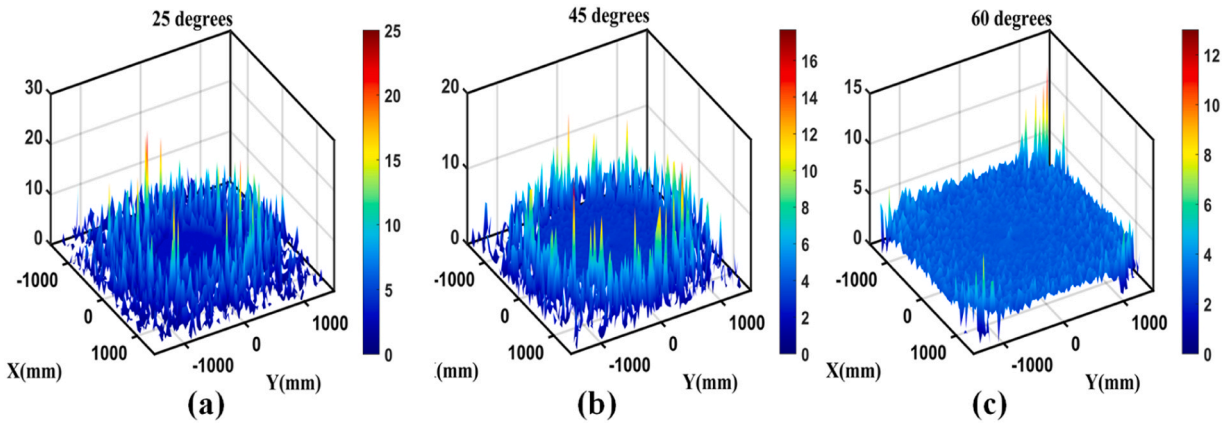

Fig. 7. The power ratio of X-ray sources with different divergences on the receiving plane: (a) 25°, (b) 45°, and (c) 60°.

The experimental results were compared with the PAM-4 scheme of the SISO system using GMXT A under the same conditions. In the experiments, the first two binary signals of length N were randomly generated. Then, the binary signals were transferred from the host computer to the FPGA (SPARTAN-7 AX7050) via Ethernet, and the two output ports *out1* and *out2* of the DAC (AN9767) module synchronously generated − 5–0 V electrical signals. Finally, the electrical signal was amplified to − 65 ∼ 0 V by the power amplifier and loaded onto the gate of the GMXT. When the grid voltage was − 65 V, no X-ray emission was observed. The X-ray exits from the two GMXTs rotate toward the center, forming an overlapping region in close proximity. The two uncorrelated OOK X-ray signals from the two GMXTs were superimposed in the intensity domain to produce the SIPAM-4 signal. To obtain the SIPAM-4 signal, GMXT A and GMXT B should ensure that the output amplitudes of the detectors meet the 1:2 requirement as closely as possible. Therefore, their filament currents were set to 1.50 A and 1.59 A, respectively.

At the receiver, the X-ray detector consists of a LYSO scintillator and a SiPM. The SIPAM-4 signal was detected by the detector after passing through the free-air channel. X-ray enters the LYSO scintillator and produces visible light by energy deposition. The visible light was then converted into an electrical signal by an SiPM (Hamamatsu, S13360–3050VE). The relationship between the tube current and detector output signal amplitude at different filament currents and anode voltages is shown in Fig. 8(c). The detector has a similar response curve at the same high anode voltage. The detected SIPAM-4 signal was captured with a digital oscilloscope (RIGOL, DS1104Z) with the sampling rate set to 5 GSa/s. The captured signal was transferred to a computer via USB flash drive for off-line demodulation and evaluation. In the XCOM system, we used the DPCA algorithm (clustering by fast search and finding density peaks) to process the data. The impact of human-selected thresholds on communication performance was mitigated by automatic clustering decisions.

4.2. BER versus anode voltage

The principle of X-ray generation by the GMXT is that electrons bomb the anode target under the acceleration of a high-voltage electric field. Therefore, the performance of the X-ray communication system is closely related to the anode voltage. The system's data rate was set to 400 kbps. Fig. 9(a) shows the relationship between the BER values of SIPAM-4 and PAM-4 and the anode voltage at a distance of 10 cm. The high-energy X-ray produced by the high anode voltage not only has a high penetration coefficient but also has a large transmitting power. As a result, the X-ray power reaching the receiver side increases, the quality of the received signal improves significantly, and the BER of the system decreases. However, when the anode voltage exceeds 55 kV, the error rate of the system increases.

Fig. 9(b)∼(e) show that the waveforms of SIPAM-4 and PAM-4 at 50 kV and 65 kV anode voltages, respectively. The intensities of S0, S1, S2, and S3 levels are 00, 01, 10, and 11 (from top to bottom), respectively. The S1 and S2 signals are superimposed to obtain the S3 signal. From Fig. 9(b) and (d), it can be seen that the signal amplitude distribution of SIPAM-4 is almost equally spaced when the anode voltage is 50 kV, while the signal amplitude of PAM-4 is not equally spaced due to the nonlinear mapping. As can be seen from Fig. 9(c) and (e), the amplitudes of both SIPAM-4 and PAM-4 signals increase when the anode voltage increases to 65 kV. Their amplitude distribution becomes uneven, especially for S2 and S3. The reason here is that the X-ray intensity is too high and enters the saturation range of the LYSO-SiPM detector (Fig. 8(c)). Choosing a suitable anode voltage avoids entering the saturation zone of the detector and reduces the impact of the nonlinear distortion of the detector on the system during communication. In addition, for XCOM in the reentry blackout region, the optimal energy of X-ray is different because the air density is different at different heights. Therefore, the choice of anode voltage also needs to consider the actual application environment.

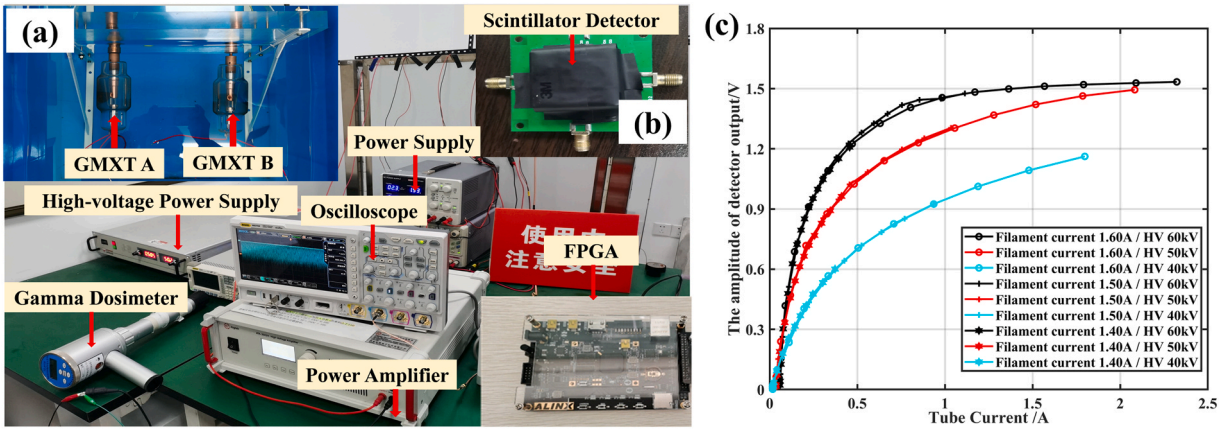

Fig. 8. Experimental setup of the 2 × 1 MISO XCOM system based on SIPAM-4 scheme. Inset: (a) GMXT array (b) the LYSO Scintillator detector. (c) The relationship between the tube current and the detector signal amplitude under different filament currents and anode voltages.

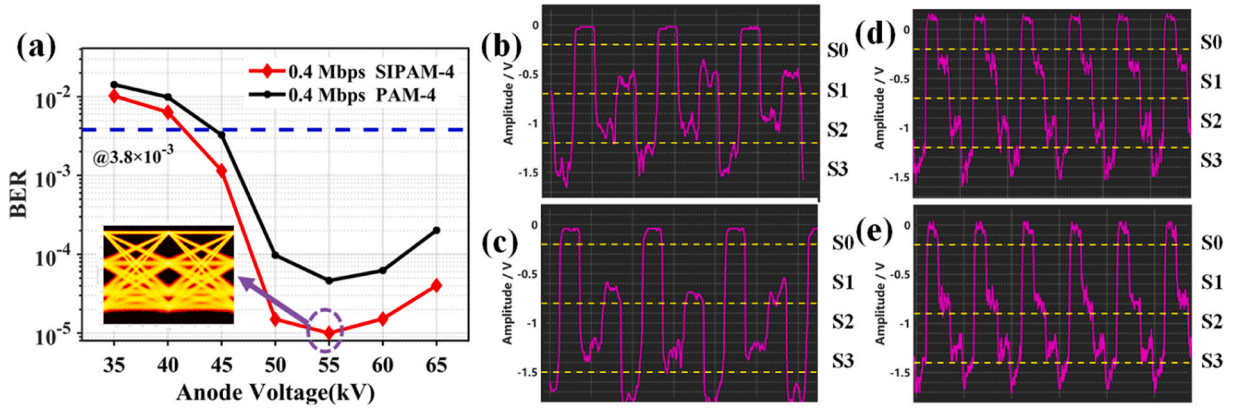

Fig. 9. (a) BER of SIPAM-4 and PAM-4 at different anode voltages. (b~c) SIPAM-4 signal waveforms at 50 kV and 65 kV. (d~e) PAM-4 signal waveforms at 50 kV and 65 kV.

4.3. BER versus position

The SIPAM-4 signal is generated by superimposing the intensity. Therefore, the performance of the received signal is extremely sensitive to the position of the detector. The detectors were placed at different positions in the XY-plane overlap region to investigate the effect on the experimental performance of the SIPAM-4 scheme (Fig. 10(a)). The data rate and anode voltage of the system were set to 400 kbps and 50 kV, respectively.

Fig. 10(b) shows the BER of SIPAM-4 and PAM-4 compared to the detector position. The BER decreases and then increases when the detector position Y changes from negative to positive. This result is consistent with the trend of the spatial distribution of the emitted X-ray in the Y-axis direction (Fig. 3(f)). The BER of the system is at its lowest when the detector is placed in the center position (Y = 0 cm).

From the experimental results, the BER performance of the SIPAM-4 scheme is improved compared with PAM-4 due to the increase in signal power. When the detector is placed within a certain range, the BER of the XCOM system is below the FEC threshold of 3.8×10^{-3}. While at a distance from the center, the BER of the system is still high, due to the fact that only 2 GMXTs were used to build the transmitter array in the experiment, which resulted in an uneven power distribution in the receiving plane and therefore did not achieve the expected effect of the simulation. In the future, a denser and interleaved array could be built to provide a more uniform X-ray power distribution at the receiving end, thus providing a larger operating area for the detector.

4.4. BER versus distance

In addition, the detectors were placed sequentially at different distances from the array GMXT to investigate the effect of distance on the system (Fig. 11(a)). Fig. 11(b) shows the BER values of SIPAM-4 and PAM-4 as a function of the distance between the X-ray array and the detector. In Fig. 11(b), it can be seen that the BER values for both modulation schemes increase with distance. This phenomenon is caused by the scattering and absorption effects of X-ray and air, resulting in a weakening of the X-ray power at the receiving end.

Interestingly, the BER level of PAM-4 is lower than that of SIPAM-4 at distances below about 9 cm. This is because for the SIPAM-4 scheme, the detector is too far from the center of the overlap region. And after 10 cm, the BER performance is improved and the distance of X-ray communication is extended because the power of the SIPAM-4 signal is higher than that of PAM-4. Because of the large size and small number of GMXTs, the constructed array is sparse, and the area of intensity superposition is limited. In the subsequent research work, by designing smaller GMXTs to construct more dense arrays and obtaining a large enough overlapping area, the defect of high BER due to low power at close distances can be compensated.

4.5. BER versus data rate

The distance between the detector and the array was 10 cm, and the anode voltage was 50 kV. Fig. 12(a) shows the BER values of SIPAM-4 and PAM-4 compared to the data rate. Both modulation schemes show a trend toward increasing BER as the data rate increases. PAM-4 can reach a rate of 1.0 Mbps before the BER exceeds the FEC target value of 3.8×10^{-3}, while SIPAM-4 can reach 1.2 Mbps. The data rate of the system increases by 20%. For PAM in XCOM, the number of photons contained in a single X-ray pulse will decrease as the data rate increases. X-ray emitted by GMXT fluctuate in intensity, making the amplitude jitter (Fig. 12(b)) of the pulse signal more severe at high speed, resulting in a low signal-to-noise ratio and a high BER.

In 2019, Russian Timofeev et al. achieved a data rate of 700 kbps using OOK modulation and demodulation techniques based on a laser-modulated X-ray system [19]. Chen et al. [8] experimentally demonstrated an improved OFDM-to-PWM scheme for XCOM that can achieve a data rate of 360 kbps. It can be seen that the proposed SIPAM-4 scheme is advantageous in terms of rate with respect to other modulation schemes.

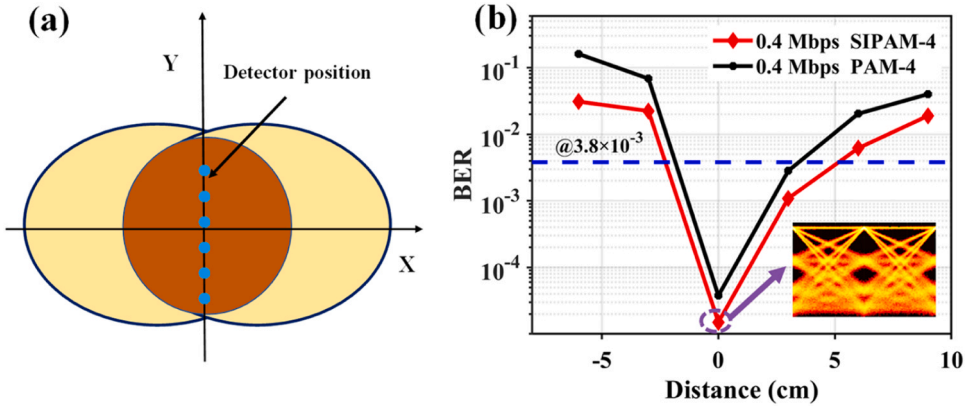

Fig. 10. (a) The placement position of the detector in the XY plane. (b) The BER of SIPAM-4 and PAM-4 at different positions of the detector in the XY plane.

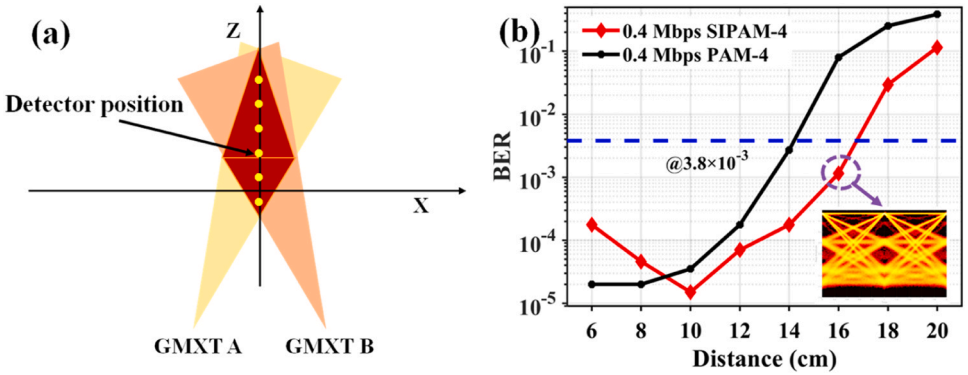

Fig. 11. (a) The placement position of the detector in the XZ plane. (b)BER of SIPAM-4 and PAM-4 at different distances between the transmitter and the receiver.

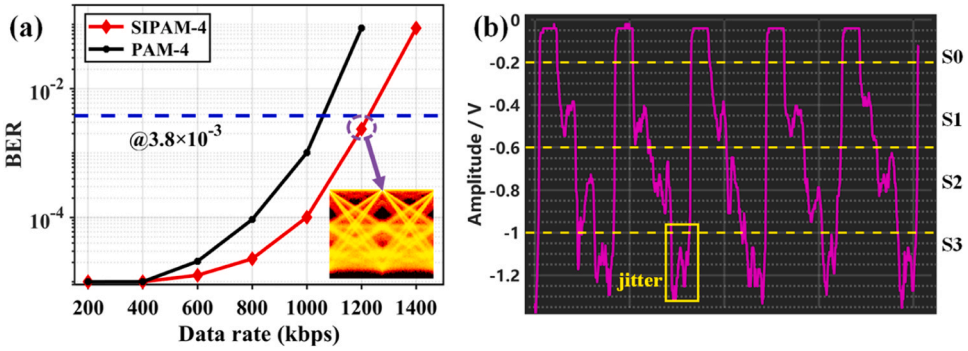

Fig. 12. (a) BER of SIPAM-4 and PAM-4 at different data rates. (b) Waveforms of SIPAM-4 at 1.2 Mbps.

Table 1
Effect of the studied factors on the measured parameters.

Parameters	Measurement Range	BER of SIPAM-4	BER of PAM-4
Anode voltage	36–65 /kV	1.52×10^{-5}~1.02×10^{-2}	4.64×10^{-5}~1.42×10^{-2}
Position	-6–9 /cm	1.50×10^{-5}~3.09×10^{-2}	3.76×10^{-5}~1.60×10^{-1}
Distance	6–20 /cm	1.50×10^{-5}~1.12×10^{-1}	2.12×10^{-5}~3.85×10^{-1}
Data rate	200–1200 /kbps	1.00×10^{-5}~2.35×10^{-3}	1.00×10^{-5}~8.75×10^{-2}

4.6. Effect of parameters

In the above experiments, we investigated the effects of anode voltage, detector position, communication distance and communication rate on the SIPAM scheme. Table 1 shows the BER ranges of both SIPAM-4 and PAM-4 modulation schemes with different test parameters. It can be seen that our SIPAM-4 scheme has better BER performance than the conventional PAM-4 under the same operating conditions. In practical applications, the SIPAM scheme has a larger operating region and increases the communication rate of the system.

5. Conclusion

XCOM, as a special optical communication technology, is expected to overcome the black barrier problem of re-entry into the atmosphere. In order to mitigate the effects of non-linear distortions at the transmitter side and reduce the complexity of the system, a pulse amplitude modulation scheme based on intensity superposition is proposed in this paper. On the one hand, numerical simulations were carried out using the Monte Carlo software Geant4 to simulate the transmission process of X-rays. The results show that the SIPAM scheme can be used in the MISO XCOM system. Furthermore, the larger the divergence angle of the GMXT, the more uniform the X-ray power distribution at the receiving end, which is expected to reduce the alignment requirements of XCOM transceivers in practical applications. On the other hand, an XCOM verification platform was built based on SIPAM-4 scheme by using two GMXTs and a LYSO-SiPM detector. The effects of data rate, distance, position and anode voltage on the BER performance of the system were experimentally investigated and compared with the conventional PAM-4 scheme. The results show that the SIPAM-4 scheme effectively reduces the impact of transmitter non-linear distortion on the system. Meanwhile, the SIPAM-4 scheme slows down the alignment requirements of the system transceiver and extends the operating region of the system due to its higher power and more uniform power distribution. When the transmission distance and anode voltage of the system are 10 cm and 50 kV respectively, a data transmission rate of 1.2 Mbps is achieved with SIPAM-4, increasing the data rate of the system by 0.2 Mbps compared with PAM-4.

The results of the study on signal modulation and system design provide preliminary guidance. However, since this study is only a preliminary validation of the proposed modulation scheme, more detailed experimental studies could be conducted in future work.

CRediT authorship contribution statement

Feixu Xiong: Conceptualization, Methodology, Visualization, Writing – original draft. **Yunpeng Liu**: Supervision, Data curation, Writing – review & editing. **Xiaobin Tang**: Supervision, Project administration, Writing – review & editing. **Junqiu Yin**: Feng: Writing – review & editing. **Junxu Mu**: Writing – review & editing.

Declaration of Competing Interest

The authors declare that they have no known competing financial interests or personal relationships that could have appeared to influence the work reported in this paper.

Acknowledgments

This work was supported by the Foundation of Graduate Innovation Center in NUAA (Grant No. xcxjh20210614).

References

[1] B.L. Henke, E.M. Gullikson, J.C. Davis, X-ray interactions: photoabsorption, scattering, transmission, and reflection at E= 50-30,000 eV, Z= 1-92[J], At. Data Nucl. Data Tables 54 (2) (1993) 181–342, https://doi.org/10.1006/adnd.1993.1013.
[2] H. Li, X. Tang, S. Hang, et al., Potential application of X-ray communication through a plasma sheath encountered during spacecraft reentry into earth's atmosphere[J], J. Appl. Phys. 121 (12) (2017), 123101, https://doi.org/10.1063/1.4978758.
[3] Y. Li, T. Su, L. Sheng, et al., X-ray transmittance characteristics and potential communication in re-enter plasma sheath[J], Optik 197 (2019), 162917, https://doi.org/10.1016/j.ijleo.2019.06.017.
[4] Y. Liu, P. Dang, X. Tang, et al., Performance analysis of LYSO–SiPM detection module for X-ray communication during spacecraft reentry blackout[J], Nucl. Instrum. Methods Phys. Res. Sect. A: Accel., Spectrometers, Detect. Assoc. Equip. 1013 (2021), 165673, https://doi.org/10.1016/j.nima.2021.165673.
[5] J. Mu, X. Tang, Y. Liu, et al., Design and performance test of pulse X-ray receiver based on LYSO-SiPM for X-ray communication[J], J. Light. Technol. 40 (13) (2022) 4217–4223, https://doi.org/10.1109/JLT.2022.3162344.
[6] W. Zhou, X. Tang, Y. Liu, et al., Power budget and performance analysis of X-ray communication during the Earth re-entry of spacecraft[J], Optik 199 (2019), 163521, https://doi.org/10.1016/j.ijleo.2019.163521.
[7] W. Lu-Qiang, S. Tong, Z. Bao-Sheng, et al., Bit error rate analysis of X-ray communication system[J], Acta Phys. Sin. -Chin. Ed. - 64 (12) (2015), 120701, https://doi.org/10.7498/aps.64.120701.
[8] W. Chen, Y. Liu, X. Tang, et al., Experimental evaluation of an OFDM-PWM-based X-ray communication system[J], Opt. Express 29 (3) (2021) 3596–3608, https://doi.org/10.1364/OE.415291.
[9] M. Kong, Y. Chen, R. Sarwar, et al., Optical superimposition-based PAM-4 signal generation for visible light communication[C]//2017 16th International Conference on Optical Communications and Networks (ICOCN), IEEE (2017) 1–3, https://doi.org/10.1109/ICOCN.2017.8121223.
[10] H.M. Oubei, J.R. Duran, B. Janjua, et al., 4.8 Gbit/s 16-QAM-OFDM transmission based on compact 450-nm laser for underwater wireless optical communication[J], Opt. Express 23 (18) (2018) 23302–23309, https://doi.org/10.1109/ICOCN.2017.8121223.
[11] J. Xu, Y. Song, X. Yu, et al., Underwater wireless transmission of high-speed QAM-OFDM signals using a compact red-light laser[J], Opt. Express 24 (8) (2016) 8097–8109, https://doi.org/10.1364/OE.24.008097.

[12] N. Chi, M. Zhang, Y. Zhou, et al., 3.375-Gb/s RGB-LED based WDM visible light communication system employing PAM-8 modulation with phase shifted Manchester coding[J], Opt. Express 24 (19) (2016) 21663–21673, https://doi.org/10.1364/OE.24.021663.
[13] G. Stepniak, L. Maksymiuk, J. Siuzdak, 1.1 GBIT/S white lighting LED-based visible light link with pulse amplitude modulation and Volterra DFE equalization [J], Microw. Opt. Technol. Lett. 57 (7) (2015) 1620–1622, https://doi.org/10.1364/OE.24.021663.
[14] O. Ozolins, X. Pang, M.I. Olmedo, et al., 100 GHz externally modulated laser for optical interconnects[J], J. Light. Technol. 35 (6) (2017) 1174–1179, https://doi.org/10.1109/JLT.2017.2651947.
[15] Z. Feng, Y. Liu, J. Mu, et al., Optimization and testing of groove-shaped grid-controlled modulated X-ray tube for X-ray communication[J], Nucl. Instrum. Methods Phys. Res. Sect. A: Accel., Spectrometers, Detect. Assoc. Equip. 1026 (2022), 166218, https://doi.org/10.1016/j.nima.2021.166218.
[16] C. Xi, A. Mirvakili, V.J. Koomson, A visible light communication system demonstration based on 16-level pulse amplitude modulation of an LED array[C]//2012 Symposium on Photonics and Optoelectronics, IEEE (2012) 1–4, https://doi.org/10.1109/SOPO.2012.6271071.
[17] M. Kong, Y. Chen, R. Sarwar, et al., Underwater wireless optical communication using an arrayed transmitter/receiver and optical superimposition-based PAM-4 signal[J], Opt. Express 26 (3) (2018) 3087–3097, https://doi.org/10.1364/OE.26.003087.
[18] M. Shi, M. Zhang, F. Wang, et al., Equiprobable pre-coding PAM7 modulation for nonlinearity mitigation in underwater 2× 1 MISO visible light communications [J], J. Light. Technol. 36 (22) (2018) 5188–5195, https://doi.org/10.1109/JLT.2018.2871078.
[19] G.A. Timofeev, N.Petrakov Potrakhov, A.I. Nechaev, Experimental research of the x-ray communication system. AIP Conference Proceedings, AIP Publishing LLC,, 2019, 020020, https://doi.org/10.1063/1.5095749.